Siegfried Ussar,[1,2,3] Max-Felix Haering,[1,4] Shiho Fujisaka,[1,5] Dominik Lutter,[3,6] Kevin Y. Lee,[1,7,8] Ning Li,[9] Georg K. Gerber,[9] Lynn Bry,[9] and C. Ronald Kahn[1]

Regulation of Glucose Uptake and Enteroendocrine Function by the Intestinal Epithelial Insulin Receptor

Diabetes 2017;66:886–896 | DOI: 10.2337/db15-1349

Insulin receptors (IRs) and IGF-I receptors (IGF-IR) are major regulators of metabolism and cell growth throughout the body; however, their roles in the intestine remain controversial. Here we show that genetic ablation of the IR or IGF-IR in intestinal epithelial cells of mice does not impair intestinal growth or development or the composition of the gut microbiome. However, the loss of IRs alters intestinal epithelial gene expression, especially in pathways related to glucose uptake and metabolism. More importantly, the loss of IRs reduces intestinal glucose uptake. As a result, mice lacking the IR in intestinal epithelium retain normal glucose tolerance during aging compared with controls, which show an age-dependent decline in glucose tolerance. Loss of the IR also results in a reduction of glucose-dependent insulinotropic polypeptide (GIP) expression from enteroendocrine K-cells and decreased GIP release in vivo after glucose ingestion but has no effect on glucagon-like peptide 1 expression or secretion. Thus, the IR in the intestinal epithelium plays important roles in intestinal gene expression, glucose uptake, and GIP production, which may contribute to pathophysiological changes in individuals with diabetes, metabolic syndrome, and other insulin-resistant states.

The intestinal mucosa consists of a single layer of rapidly proliferating, specialized epithelial cell types (1,2). The uptake of various classes of nutrients and other substances through enterocytes depends on a multitude of receptors and transporters (3), determining their preferential site of absorption. Glucose is predominantly absorbed in the proximal small intestine, whereas lipids are absorbed throughout the small intestine (4,5). The large intestine, on the other hand, is the major site of water absorption and the primary site for microbially mediated hindgut fermentation and production of short-chain fatty acids (6).

Uptake of glucose in the small intestine is facilitated via the sodium–glucose cotransporter 1 (SGLT1), which is constitutively localized to the luminal membrane of the enterocytes (4,7,8). SGLT1-dependent glucose uptake is also important in enteroendocrine cells, where glucose or its metabolites stimulate the expression and secretion of glucose-dependent insulinotropic polypeptide (GIP) and glucagon-like peptide 1 (GLP-1) (9,10). Export of glucose from the basolateral side of enterocytes into the circulation, on the other hand, is mediated primarily via GLUT2 (11).

A major function of insulin in peripheral tissues is to stimulate glucose uptake via translocation of GLUT4 transporters to the plasma membrane (12). However, the role of insulin action in intestinal glucose absorption is unclear. Studies in patients with diabetes and in vitro have shown conflicting results, with insulin signaling implicated in both increased and decreased glucose uptake from the intestinal lumen (13–17). Several studies in rodents have suggested

[1]Section on Integrative Physiology and Metabolism, Joslin Diabetes Center, Harvard Medical School, Boston, MA
[2]JRG Adipocytes and Metabolism, Institute for Diabetes and Obesity, Helmholtz Diabetes Center at Helmholtz Center Munich, Neuherberg, Germany
[3]German Center for Diabetes Research (DZD), Neuherberg, Germany
[4]Division of Clinical Chemistry and Pathobiochemistry, Department of Internal Medicine IV, University Hospital Tübingen, Tübingen, Germany
[5]First Department of Internal Medicine, University of Toyama, Toyama, Japan
[6]Institute for Diabetes and Obesity, Helmholtz Diabetes Center at Helmholtz Center Munich, Neuherberg, Germany
[7]Department of Biomedical Sciences, Heritage College of Osteopathic Medicine, Ohio University, Athens, OH
[8]The Diabetes Institute, Ohio University, Athens, OH
[9]Center for Clinical and Translational Metagenomics, Department of Pathology, Brigham and Women's Hospital, Harvard Medical School, Boston, MA
Corresponding author: C. Ronald Kahn, c.ronald.kahn@joslin.harvard.edu.

Received 28 September 2015 and accepted 11 January 2017.
This article contains Supplementary Data online at http://diabetes.diabetesjournals.org/lookup/suppl/doi:10.2337/db15-1349/-/DC1.
S.U. and M.-F.H. contributed equally to this work.

an additional role of the insulin receptor (IR) and the closely related IGF-I receptor (IGF-IR) in promoting gut maturation and development (18–22). However, previous studies in mice with an IR knockout in the intestinal epithelium did not identify any major role of the IR in glucose or lipid metabolism (23), nor were any changes in proliferation or intestinal length detected upon tamoxifen-induced deletion of the IGF-IR (24). In these studies, however, glucose uptake and the effects of aging were not directly assessed, and the IGF-IR deletion was performed in young adult mice after intestinal development was complete. Thus, the exact roles of early deletion of the IR and IGF-IR in these important intestinal functions still remain unclear.

To investigate the roles of the IR and IGF-IR in intestinal epithelial function in greater detail, we therefore established mice with a specific deletion of the IR or the IGF-IR in intestinal epithelial cells using villin-cre and observed them throughout life and in response to a high-fat diet (HFD) challenge. We find that developmental deletion of the IGF-IR did not result in any physiological abnormalities or retardation in intestinal growth and development. In contrast, developmental deletion of the IR results in altered gene expression reduced glucose absorption, a decrease in GIP expression, and glucose-dependent release from enteroendocrine K-cells. In this manner, the intestinal IR plays a specific role in fine-tuning glucose homeostasis by regulating glucose uptake and glucose-dependent incretin release.

RESEARCH DESIGN AND METHODS

Animals and Diets

IR and IGF-IR fl/fl mice on a C57BL/6 genetic background were bred with villin-cre mice to obtain IR fl/fl villin-cre$^+$ (VILIRKO) and IGF-IR villin-cre$^+$ (VILIGFRKO) mice and their respective fl/fl littermate controls. Mice were allowed ad libitum access to water and chow diet (CD) containing 22% calories from fat (9F 5020; PharmaServ) or HFD containing 60% calories from fat (D12492; Open Source Diets). All mice were housed in a facility with a 12-h light/dark cycle in a temperature-controlled room. Animal care and study protocols were approved by the Animal Care Committee of Joslin Diabetes Center and were in accordance with the National Institutes of Health guidelines.

Metabolic Analysis

Twelve-week-old male VILIRKO and control mice were individually housed and evaluated for ambulatory activity using an OPTO-M3 sensor system (CLAMS; Columbus Instruments). Indirect calorimetry was measured on the same mice using an open-circuit Oxymax system (Columbus Instruments). After a 48-h acclimation period, exhaust air was sampled for 60 s every 12 min in each cage consecutively for 72 h with ad libitum access to food to determine O_2 consumption and CO_2 production.

Intraperitoneal glucose tolerance tests (2 g/kg body wt), oral glucose tolerance tests (2 g/kg body wt), and insulin tolerance tests (1.25 units/kg body wt) were performed in unrestrained conscious male mice after a 16- and 4-h fast for glucose and insulin tolerance tests, respectively. Oral glucose tolerance tests were performed by gavaging glucose directly into the stomach.

Gene Expression

Total RNA was extracted using a RNeasy Mini Kit (QIAGEN), and 1 μg RNA was used for reverse transcription (Applied Biosystems). SYBR green–based quantitative real-time PCR (qPCR) was performed in a CFX Real-Time PCR system (Bio-Rad) using 300 nmol/L gene-specific primers with an initial denaturation at 95°C for 10 min, followed by 40 PCR cycles, each consisting of 95°C for 15 s and 60°C for 1 min. mRNA expression was calculated relative to TATA binding protein. Primer sequences are presented in Supplementary Table 1.

Microarray Processing and Data Analysis

Total RNA extracted from jejunal epithelial cells from 6-month-old CD-fed control and VILIRKO mice was analyzed using Affymetrix mouse gene 2.0 chips. Affymetrix CEL files were preprocessed using the Bioconductor R package affy (25). Expression values were calculated using the RMA algorithm. Gene names and gene symbols for each probeset were derived from the Bioconductor mogene20sttranscriptcluster.db package version 8.4.0. Gene expression was filtered to remove the lowest 10% of all absolute expression values. Transcripts with a variance <0.05 were also removed. Non–protein-coding genes were excluded using biomaRt (26). Differential expression was estimated using one-way ANOVA with an α of $P < 0.05$ and a minimum 1.5-fold change of expression. KEGG (Kyoto Encyclopedia of Genes and Genomes) enrichment analysis was performed using a hypergeometric distribution test. Filtering of gene expression and statistics were performed using MATLAB 2016b.

Western Blot

Intestinal epithelial cells were isolated after 1 h of incubation of the small intestine in chelating solution as previously described (27). Isolated intestinal epithelial cells were maintained in DMEM in suspension for 30 min in a cell culture incubator prior to stimulation. Stimulations were stopped with ice-cold DMEM and immediate centrifugation at 4°C. Proteins were extracted from cells in lysis buffer (25 mmol/L Tris-HCl, pH 7.4, 150 mmol/L NaCl, 1% NP-40, 1 mmol/L EDTA, 5% glycerol, 0.1% SDS) containing protease and phosphatase inhibitors. Thirty micrograms of protein were subjected to SDS-PAGE and transferred to polyvinylidene fluoride membranes. The following antibodies were used: IR β-subunit, extracellular signal–regulated kinase (ERK), phospho-ERK, AKT, phospho-AKT, IGF-IR β-subunit, and phospho-IR/IGF-IR (1:1,000; all from Cell Signaling Technologies); and SGLT1 (1:500; Abcam).

Immunofluorescence

Immunofluorescence was performed on formalin-fixed sections using the following antibodies: E-Cadherin (1:500;

Life Technologies), Ki-67 (1:200; Cell Signaling Technologies), SGLT1 (1:50; Abcam), GLP-1 (1:500; Phoenix Pharmaceuticals), and GIP (1:500; Phoenix Pharmaceuticals), which were detected with Alexa Fluor 594– or Alexa Fluor 488–conjugated secondary antibodies (1:500; Invitrogen).

Glucose Uptake Assay

For ex vivo glucose uptake, jejunal epithelial cells were isolated on ice and incubated for 30 min in 37°C in 2.8 mmol/L glucose DMEM, penicillin, and streptomycin, and then resuspended in Krebs-Ringer buffer containing 2 mmol/L pyruvate and incubated for 30 min in 37°C. [^{3}H]2-deoxy-D-glucose (2-DOG) (PerkinElmer) was then added for 10 min in 37°C (on ice for control) in the presence of the absence of insulin. Radioactivity was assayed in samples and normalized to protein concentration. Results are shown as the fold change between control and VILIRKO cells.

For the in vivo glucose uptake assay, mice were fasted for 16 h and gavaged with 2 g/kg body wt glucose plus 2.3 μL/g body wt [^{14}C]3-*O*-methyl-D-glucose (3-OMG) (50 μCi/1.85 MBq; PerkinElmer). A parallel group of mice was gavaged with 1 g/kg phloridzin diluted in saline 15 min prior to glucose gavage, and radioactivity was assayed in blood. Background counts, assessed in samples without radioactivity, were subtracted from each sample.

Microbiome Analysis

A multiplexed amplicon library covering the 16*S* ribosomal DNA gene V4 region was generated from mouse stool sample DNA. Bacterial genomic DNA was extracted using the Power-Fecal DNA Isolation Kit (MO BIO Laboratories) with modification of the library preparation following the protocol of Kozich et al. (28). Aggregated libraries were sequenced with paired-end 300–base pair reads made on the Illumina MiSeq platform at the Molecular Biology Core Facilities at the Dana-Farber Cancer Institute. Raw sequencing reads were processed using the mothur software package (29), and custom Python scripts, which perform denoising, quality filtering, alignment against the ARB Silva reference database of 16S ribosomal DNA gene sequences, and clustering into operational taxonomic units at 97% identity. A measure of overall microbial community diversity, the Shannon entropy (30), was calculated for the samples. To statistically test for differences in the relative abundances of microbial taxa (phylum/genera) between cohorts, the DESeq2 (31,32) software package was used.

Other Assays and Statistics

ELISAs for obtaining insulin and incretin serum levels were performed by the Joslin Diabetes Research Center Specialized Assay Core. Bomb calorimetry of fecal calorie content was performed by the Central Analytical Laboratory at the University of Arkansas. All differences, except the Affymetrix chip analysis, for which the statistical analysis is described above, were analyzed by ANOVA or Student *t* test and were considered significant at $P < 0.05$.

RESULTS

Intestinal Epithelial Insulin/IGF-I Signaling Is Dispensable for Intestinal Growth and Development

To determine the roles of the intestinal epithelial IR and IGF-IR in intestinal development, growth, and metabolic function, we created mice with an intestinal epithelial–specific deletion of the IR or IGF-IR using Cre recombinase under the control of the murine villin promoter (hereafter referred to as VILIRKO and VILIGFRKO mice, respectively). Villin-cre induces specific recombination in all epithelial cell types of the small and large intestine (33). To assess the efficiency of the knockout, IR mRNA was assessed in isolated epithelial cells from the duodenum, jejunum, and ileum of control (fl/fl littermates) and VILIRKO mice (Fig. 1*A*, left panel). Consistent with previous studies (34–36), IR was expressed at the highest level in the duodenum followed by the jejunum, with 50% lower levels in the ileum. The colon had levels similar to those in the duodenum. VILIRKO mice had >90% reductions in IR mRNA in all segments of the small intestine and colon (Fig. 1*A*). This virtually complete loss of IR expression was confirmed at the protein level by Western blot analysis (Fig. 1*B*). In control mice, mRNA expression of the IGF-IR was highest in the colon (Supplementary Fig. 1*A*), and both the jejunum and colon showed >90% reduction in VILIGFRKO mice compared with controls (Supplementary Fig. 1*B*).

To investigate the effects of the loss of the IR on insulin signaling in the intestine, epithelial cells were isolated from the jejunum of control and VILIRKO mice, stimulated for 10 min with insulin or IGF-I (100 nmol/L), and analyzed for activation of the IR/IGF-IR and ERK (Fig. 1*C* and *D*). Consistent with Fig. 1*B*, there was a marked reduction in IR protein in the VILIRKO epithelial cells. In controls, in vitro stimulation with insulin led to a robust increase in phosphorylation of the IR, and this was completely lost in cells obtained from VILIRKO mice, indicating that preparation did not impair cell viability and that cells were still responsive to insulin/IGF-I (Fig. 1*C*). This was paralleled by decreases in both basal and stimulated ERK phosphorylation. Stimulation of cells with 100 nmol/L IGF-I also showed a reduced phosphorylation of ERK, despite somewhat increased phosphorylation of the IGF-IR, suggesting that the loss of the IR probably also affected postreceptor signaling.

VILIRKO mice showed weight gain over 18 weeks that was comparable to that in controls on a standard CD (22% of kcal from fat) and had comparable liver, subcutaneous fat, and perigonadal fat pad weights (Supplementary Fig. 1*C*). Control and VILIRKO mice gained significantly more and equivalent weights on an HFD (60% of kcal from fat) (Fig. 1*E*) and had comparable increases in liver and adipose tissue weight (Supplementary Fig. 1*C*). There was also no difference in food intake or fecal caloric content between control and VILIRKO mice (Fig. 1*F* and Supplementary Fig. 1*D*). Similarly, VILIGFRKO

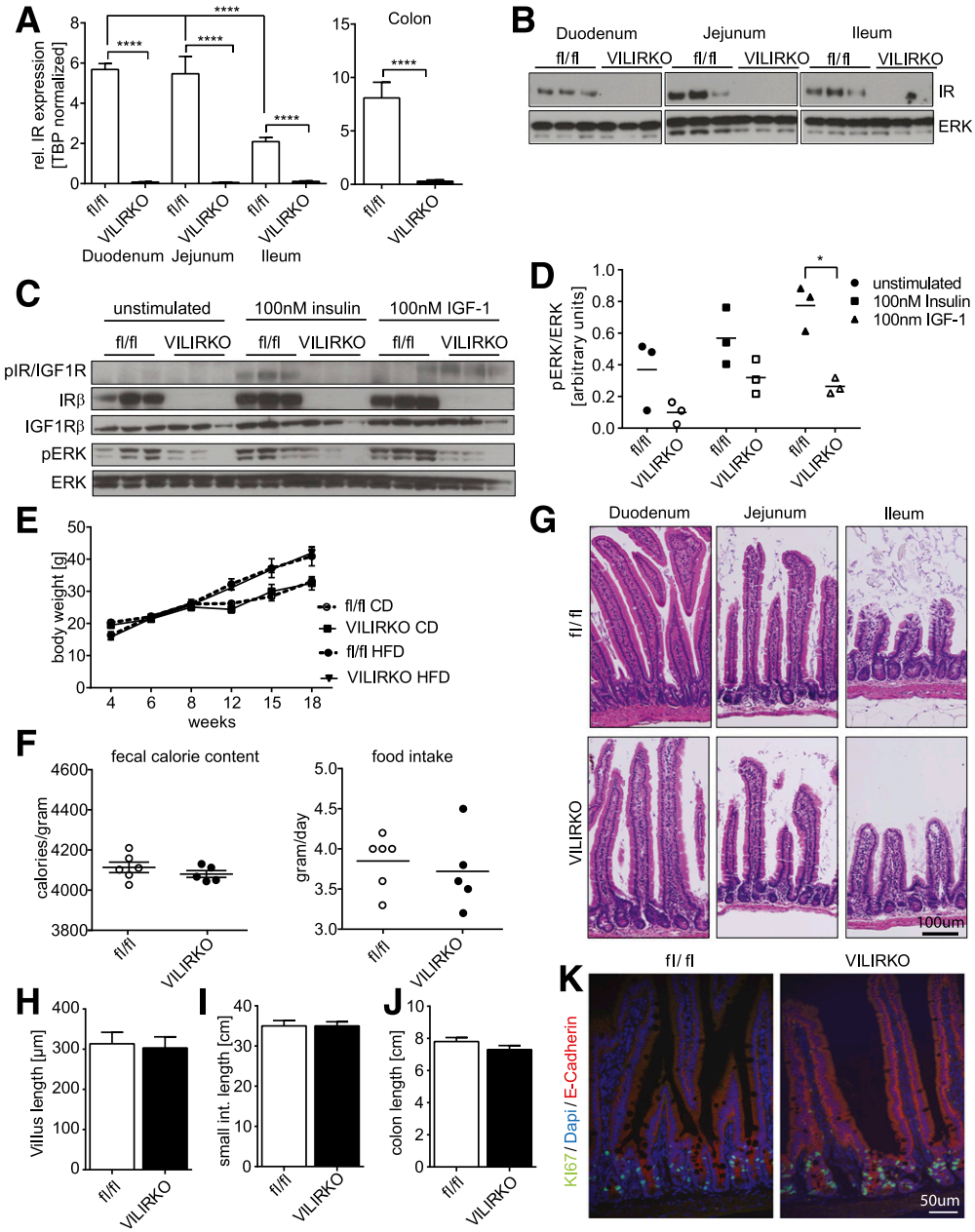

Figure 1—Intestinal epithelial insulin signaling is dispensable for normal growth and intestinal development. *A*: Expression levels of IR in the intestine of VILIRKO and control mice. IR mRNA was measured by qPCR of RNA from isolated epithelial cells of the duodenum, jejunum, ileum, and colon of 18-week-old male VILIRKO and control (fl/fl) mice on CD. In all panels, data are shown as mean ± SEM (n = 5–7). ****P < 0.0001 (two-way ANOVA, Tukey post hoc test and unpaired t test [colon]). *B*: Western blot for IR β-subunit from isolated intestinal epithelial cells from duodenum, jejunum, and ileum of 18-week-old male VILIRKO and control (fl/fl) mice on CD. ERK protein levels were used as the loading control. *C*: Western blot analysis of IR β-subunit, IGF-IR, phosphorylated (p) IR/IGF-IR, ERK, and pERK from isolated jejunal epithelial cells of 12-week-old male VILIRKO and fl/fl mice on CD. Cells were untreated, stimulated with 100 nmol/L insulin, or stimulated with 100 nmol/L IGF-I for 10 min. *D*: Quantification of the pERK/ERK ratio from blots shown in *C*. *P < 0.05 (two-way ANOVA, Tukey post hoc test). *E*: Body weights from male VILIRKO and fl/fl mice fed either CD or HFD for the indicated times (n = 5–7). *F*: Fecal calorie content was measured by bomb calorimetry from feces and average food intake per day measured over 5 days from 12-week-old male CD-fed VILIRKO and fl/fl mice (n = 5–6). *G*: Hematoxylin-eosin staining of duodenum, jejunum, and ileum from 18-week-old male VILIRKO and fl/fl mice on CD. *H*: Crypt-villus length was measured with ImageJ software on images from histological sections of the jejunum from 18-week-old male VILIRKO and fl/fl mice on CD. Length was measured for at least 30 crypt-villi in each section (n = 5). Small intestine (*I*) and colon (*J*) length from 18-week-old male VILIRKO and fl/fl mice on a CD (n = 4–5). *K*: Representative staining for Ki-67 (green), E-Cadherin (red), and DAPI (blue) of the jejunum from 18-week-old male VILIRKO and fl/fl mice on CD. rel., relative.

mice showed no difference in body weight or weight gain and no change in liver weight during the 3-month study period (Supplementary Fig. 1*F* and *G*).

Histological examination of the jejuna of control and VILIRKO mice revealed normal intestinal structure with no difference in the length of the crypt-villus axis (Fig. 1*G* and *H*). Small and large intestinal lengths were also normal in both VILIRKO (Fig. 1*I* and *J*) and VILIGFRKO mice (Supplementary Fig. 1*G*). Immunofluorescence staining for Ki-67 in jejunal sections of VILIRKO mice indicated no differences in proliferation (Fig. 1*K*), as previously described (23). Thus, neither the IR nor the IGF-IR is essential for normal growth and development of the intestinal epithelium.

Loss of Intestinal Epithelial IR Improves Age-Dependent Glucose Intolerance and Glucose Transporter Activity

Previous studies (13–17,23) using a variety of approaches have shown inconsistent effects of insulin on glucose uptake from the intestine. In VILIRKO mice, results of oral glucose tolerance tests (OGTTs) at 8 weeks were not different from those for controls (Fig. 2*A*). However, as mice matured, there was a natural decline in glucose tolerance in control mice, whereas VILIRKO mice maintained good glucose tolerance, such that by 12 weeks of age VILIRKO mice exhibited slightly better glucose tolerance than controls (Fig. 2*A*). This effect further increased by 20 weeks of age with VILIRKO mice demonstrating significantly lower glucose levels during an OGTT, resulting in a 20% reduction in the area under the glucose curve ($P = 0.02$) (Fig. 2*A*). The effect of the improved glucose tolerance was even greater when mice were challenged with an HFD with a 34% reduction in the area under the glucose curve in VILIRKO mice compared with controls ($P = 0.009$) (Fig. 2*A*). In contrast, OGTTs in 19-week-old VILIGFRKO mice showed no difference between groups (Fig. 2*B*), indicating that this effect was IR specific. Likewise, no differences were observed in blood glucose levels or intraperitoneal glucose tolerance test results between 18-week-old random-fed VILIRKO and control mice (Supplementary Fig. 2*A* and *B*), indicating that the improved glucose handling in these mice was due to an effect of IR action on glucose uptake from the intestine. Serum insulin levels in VILIRKO mice on a CD or HFD were not significantly different from those of controls (Supplementary Fig. 2*C*), nor was there any difference in insulin tolerance between VILIRKO and VILIGFRKO mice and their respective controls (Supplementary Fig. 2*D* and *E*). Assessment of body composition using DEXA scans and other metabolic parameters, like O_2 consumption, CO_2 production, respiratory exchange ratio, as well as mean activity, measured in CLAMS metabolic cages, also did not reveal a significant difference in metabolic rates, bone mineral density, lean mass, and fat mass between VILIRKO and control mice (Supplementary Fig. 3).

The primary transporters involved in glucose uptake from the intestinal lumen into the epithelial cells are SGLT1 and, upon high luminal glucose concentrations, GLUT2 (37,38). To assess transporter activity in vivo, we performed an oral glucose uptake assay in 8-week-old mice using the nonmetabolizable glucose analog 3-OMG. 3-OMG was used instead of 2-DOG, since 3-OMG cannot be phosphorylated and retained within cells, allowing the quantification of tracer uptake into blood. To assess the amount of SGLT1-mediated glucose uptake, separate cohorts of control and VILIRKO mice were gavaged with the SGLT1/SGLT2 inhibitor phloridzin dehydrate (phloridzin; 1 g/kg body wt) prior to the oral glucose administration. At this young age, there were no differences in blood glucose levels between the VILIRKO and control mice during the OGTT (Fig. 2*C*, solid line with filled circles and

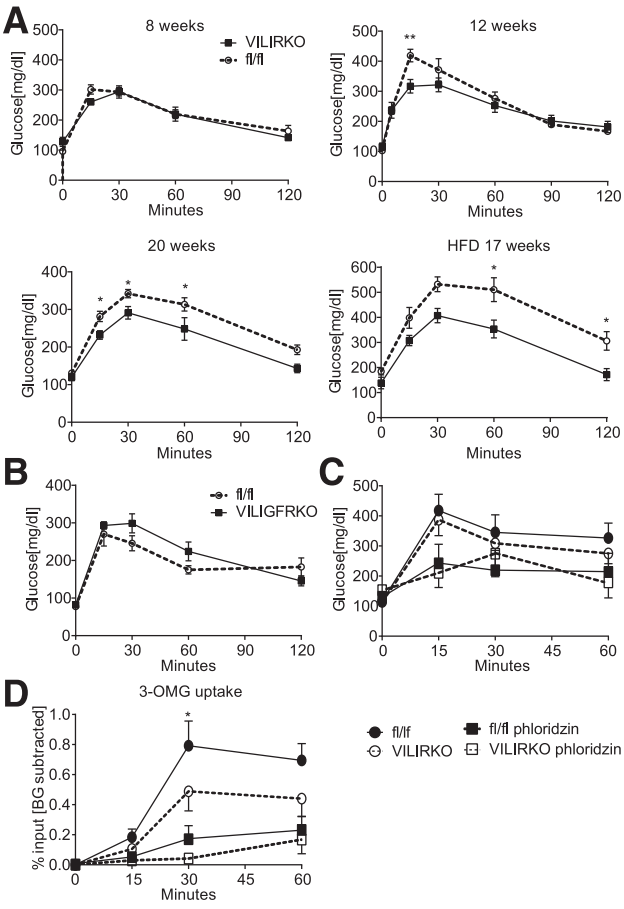

Figure 2—Loss of intestinal epithelial IR improves glucose intolerance and decreases glucose uptake in intestinal epithelial cells. *A*: OGTTs of 8-, 12-, and 20-week-old male VILIRKO and fl/fl mice on CD and 17-week-old male VILIRKO and fl/fl mice on HFD. Data are shown as mean ± SEM. ($n \geq 5$ animals/group; repeated-measures two-way ANOVA with Sidak multiple-comparison test [12 and 17 weeks] and uncorrected Fisher least significant difference for 20 weeks; $^*P < 0.05$, $^{**}P < 0.01$). *B*: OGTT of 8-week-old male VILIGFRKO and fl/fl mice on CD ($n = 4$–5). Blood glucose (*C*) and 3-OMG (*D*) levels during an in vivo oral glucose uptake assay in 8-week-old male VILIRKO and fl/fl mice on CD. Indicated mice were gavaged with 100 mg/kg phloridzin 15 min before the administration of the glucose load ($n = 3$–5). Repeated-measures two-way ANOVA with Dunnett multiple-comparison test, $^*P < 0.05$. BG, background counts.

dashed line with solid squares). In control mice, blood levels of 3-OMG peaked at 30 min, and this was reduced by ~80% in the phloridzin-pretreated mice (Fig. 2*D*, solid line with filled squares and dashed line with empty squares), which is consistent with SGLT1 being the major intestinal glucose transporter. In the VILIRKO mice, there was an ~50% decrease in total 3-OMG uptake, with a proportional decrease after phloridzin pretreatment (Fig. 2*D*, solid line with open symbol and dashed line with open symbol). After phloridzin pretreatment, no statistically significant differences between control and VILIRKO mice could be observed. Together, these data indicate that SGLT1 is most likely the primary transporter responsible for the change in glucose uptake from the intestine of VILIRKO mice; however, with a possibility of degradation of phloridzin to phloretin, we cannot exclude a role of GLUT2 in the observed phenotype.

IR Regulates Glucose Transporter Activity but Not Expression

Glucose uptake into isolated jejunal epithelial cells in vitro was assessed using 2-DOG, which, after transport into cells, is phosphorylated and retained. Compared with controls, 2-DOG uptake was >40% decreased in VILIRKO mice. Treatment of these cells with 100 nmol/L insulin for 10 min did not increase glucose uptake in either control or VILIRKO cells (Fig. 3*A*). Together, these results indicate that the intestinal epithelial cell is insulin responsive in terms of signaling and that the IR plays a role in SGLT1/GLUT2-mediated glucose uptake. Gene expression analysis of isolated cells from the duodenum, jejunum, and ileum showed that SGLT1 and GLUT2 mRNAs were highest in the duodenum and jejunum, but with no significant differences in the expression of either transporter between VILIRKO and control mice (Fig. 3*B*). Likewise, there was no significant difference in SGLT1 expression at the protein level (Fig. 3*C*) and no differences in the localization of SGLT1 by immunofluorescence staining on jejunal sections (Fig. 3*D*).

To identify additional genes dysregulated in VIRLIKO mice that might play a role in the altered glucose uptake, we measured gene expression profiles using microarrays. We found 132 significantly regulated protein-coding genes (Supplementary Fig. 4*A* and *B*) (ANOVA, $P < 0.05$, fold change >1.5). Unsupervised KEGG pathway enrichment analysis revealed 26 significantly enriched pathways (Fig. 3*E* and Supplementary Table 2). Seven of these pathways were consistently upregulated, whereas nine pathways were consistently downregulated. The remaining 10 pathways showed significant gene regulation in both directions. To determine the differences potentially associated with reduced glucose transport, we used the STRING database to identify genes/proteins directly interacting with SGLT1 (Supplementary Fig. 4*C* and Supplementary Table 3). We found 10 genes predicted or validated to interact with SGLT1, of which 5 could be detected in the microarray data set. KEGG enrichment of these 11 proteins (10 interactors and SGLT1) revealed "carbohydrate digestion and absorption" as the most relevant pathway. Subsequently, we identified all genes mapping to carbohydrate digestion and metabolism and inspected their differential expression (Supplementary Fig. 4*D*). None of the 14 detected pathway members were statistically significantly regulated. However, among the nine upregulated genes, hexokinase 2 (Hk2) was upregulated, whereas the predominant isoform of glucose-6-phosphatase (G6pc) was downregulated, suggesting a diversion of glucose utilization into the intestinal epithelium of VILIRKO mice, which could contribute to the decreased release of glucose into the circulation. Exactly how altered glucose metabolism and/or reduced glucose transport in the intestines of VILIRKO mice are related to the reduction in glucose transporter activity will require further investigation.

The loss of insulin action and the decrease of glucose uptake in the VILIRKO mice could alter the intestinal milieu, resulting in changes in the composition of the gut microbial community, and this, in turn, could further indirectly impact host metabolism. We therefore performed an analysis of the gut microbiome community composition by sequencing the V4 region of the 16S rRNA gene in fecal samples of VILIRKO and control mice (16S rRNA data sets have been deposited in the European Nucleotide Archive). This did not reveal significant differences in phylogenetic diversity (Shannon Entropy) or any significant changes in the relative abundances of individual phyla (Supplementary Fig. 5*A* and *B*). There were also no significant differences between individual taxa.

Intestinal Epithelial IR Regulates GIP Expression and Secretion

Incretins like GIP and GLP-1 are important modulators of insulin secretion from the pancreatic β-cell. Incretins are released upon stimulation by glucose and other nutrients in the intestinal lumen. qPCR analysis showed that GIP mRNA was decreased by >40% in the duodenum ($P = 0.04$) and jejunum ($P = 0.007$) of VILIRKO mice, whereas proglucagon mRNA (proglucagon/Glp-1 [GCG]), the precursor for GLP-1, tended to be increased. mRNAs for peptide YY (PYY) and the enteroendocrine marker chromogranin A (CHGA) were unchanged in the VILIRKO mice (Fig. 4*A*). None of these genes, including the IR and GIP, were changed in expression in VILIGFRKO mice (Supplementary Fig. 6), so this effect was IR specific. The decreased expression of GIP correlated with a 16% ($P < 0.05$) decrease in GIP immunoreactive K-cells in VILIRKO mice compared with control (Fig. 4*B*); this occurred with no difference in the expression of CHGA (Fig. 4*A*). There was also no change in the number of L-cells (GLP-1 positive) (Fig. 4*C*). Consistent with the decreases in GIP-positive cells and GIP mRNA, VILIRKO mice had an ~30% decrease in peak serum GIP levels after acute oral glucose challenge compared with controls (Fig. 4*D*). Serum levels of other incretins, like GLP-1 and PYY, showed no difference between VILIRKO and control mice (Fig. 4*D*).

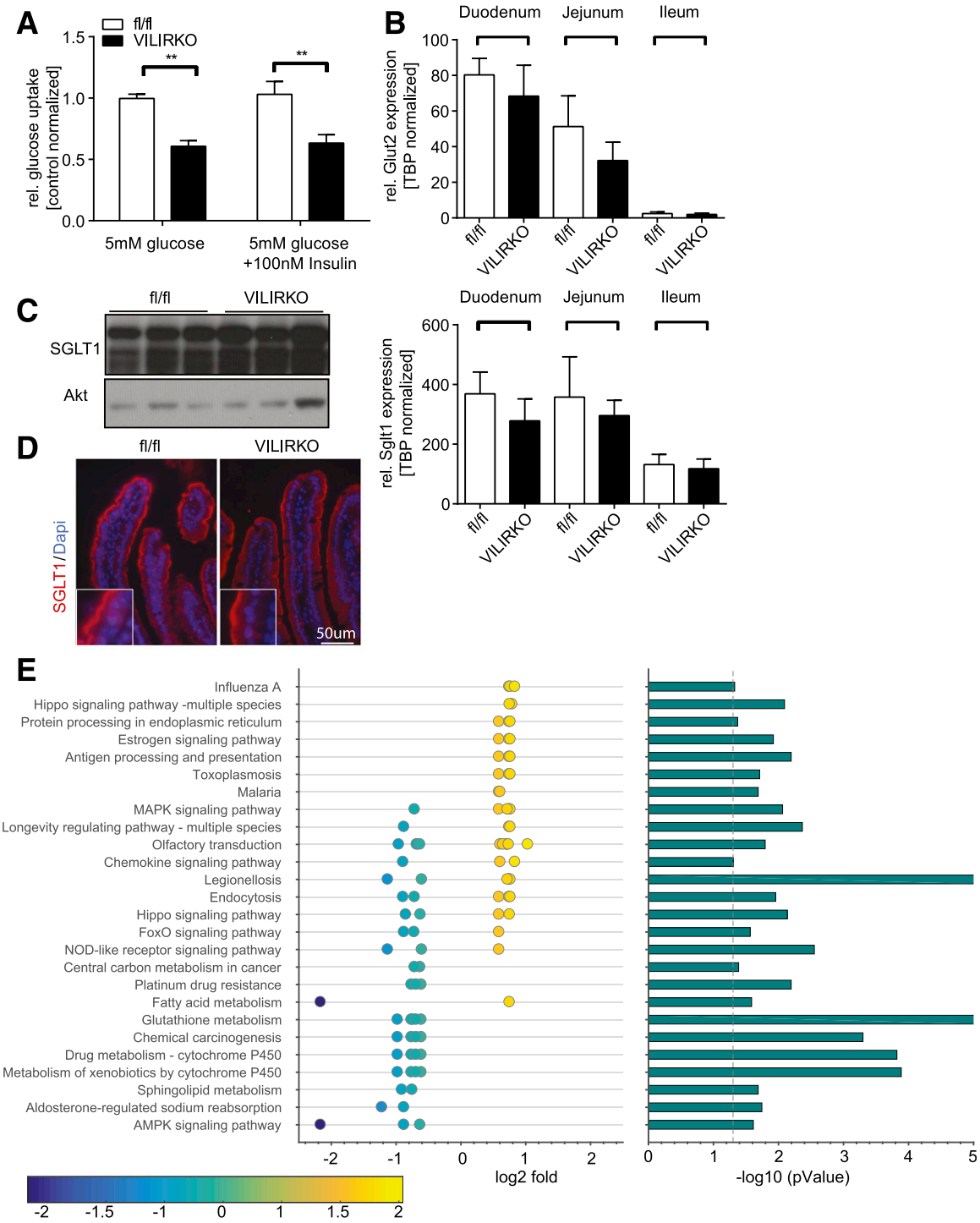

Figure 3—Intestinal epithelial IR regulates SGLT1 activity without affecting transporter expression. *A*: Ex vivo glucose uptake assay from isolated jejunal epithelial cells with 2-DOG. Uptake was measured with basal glucose and after stimulation with 100 nmol/L insulin for 10 min, as described in RESEARCH DESIGN AND METHODS. Data are shown as mean fold change ± SEM, $n = 5$ animals/group. $^{**}P < 0.01$, two-way ANOVA with Sidak multiple comparison tests. *B*: TATA binding protein (TBP) normalized mRNA expression of GLUT2 and SGLT1 measured from isolated epithelial cells of the duodenum, jejunum, and ileum of 18-week-old male VILIRKO and fl/fl mice on CD. Data are shown as mean ± SEM ($n = 5$). *C*: Western blot for SGLT1 from the duodena of 18-week-old male VILIRKO and fl/fl mice on CD. Akt was used as the loading control. *D*: Immunofluorescence for SGLT1 (red) and DAPI (blue) of jejuna from 18-week-old male VILIRKO and fl/fl mice on CD. *E*: KEGG pathway enrichment analysis, ordered according to mean $\log_2$FC expression. Log_2FC of significantly regulated pathway members is shown in the dot plot. Each row shows the $\log_2$FC expression of the respective genes that were used for enrichment analysis. The bar plot shows the $-\log_{10} P$ values for the enriched KEGG pathways. Enrichment was calculated using a hypergeometric distribution test. rel., relative.

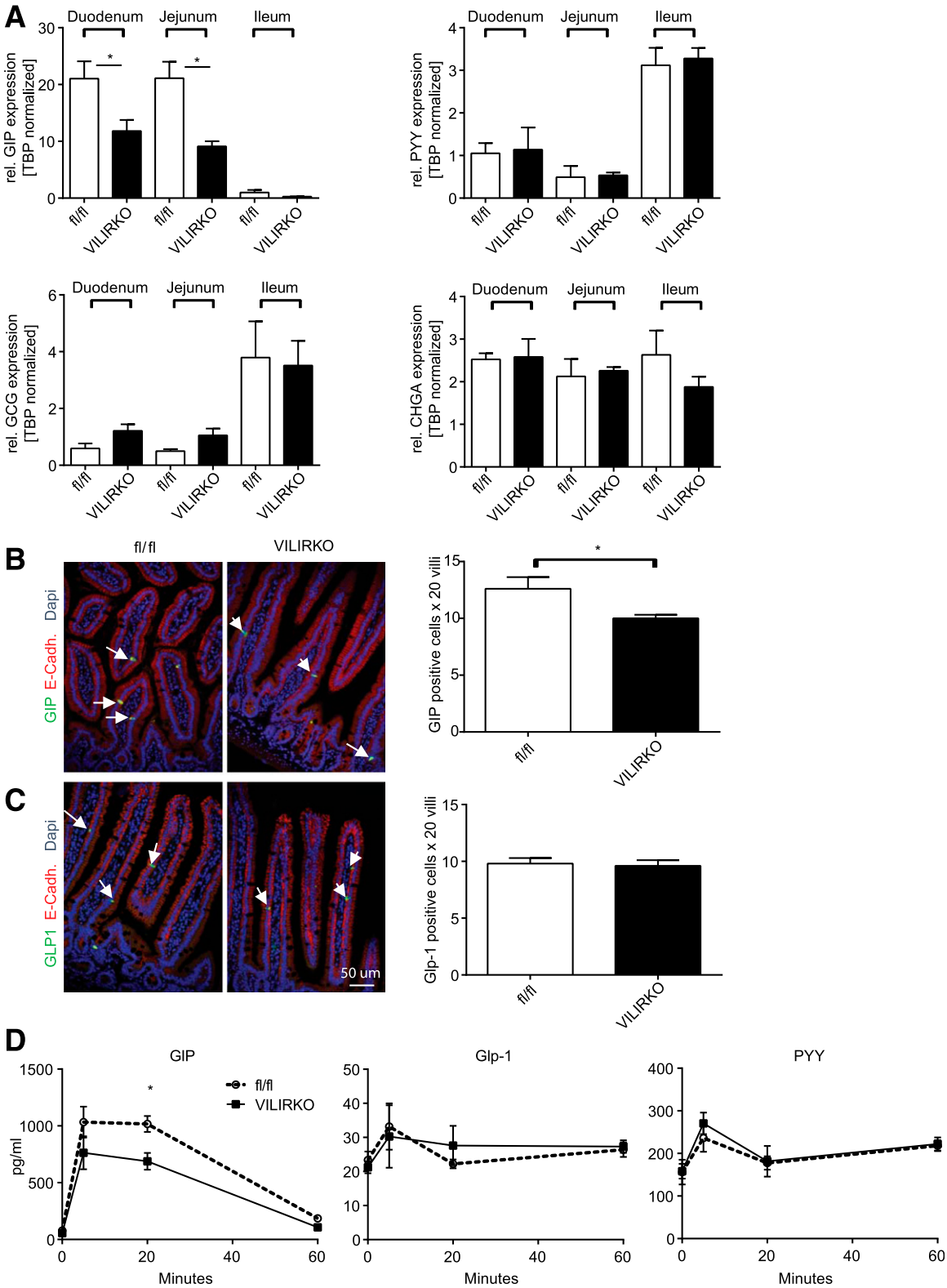

Figure 4—Intestinal epithelial IR regulates GIP expression and secretion. *A*: Expression of GIP, GCG, PYY, and CHGA mRNA from isolated epithelial cells of the duodenum, jejunum, and ileum of 18-week-old male VILIRKO and fl/fl mice on CD. Data are shown as mean ± SEM, n = 5 (unpaired Student t test). Immunofluorescence staining for GIP (green) (*B*) and GLP-1 (green) (*C*) of jejunal sections from 18-week-old male VILIRKO and fl/fl mice on CD. *B* and *C*: Quantification of GIP- and GLP-1–positive cells (arrows) from at least 40 villi on sections of the jejunum (right panels). Data are shown as mean ± SEM of positive cells/20 villi in VILIRKO and fl/fl mice on CD (*$P < 0.05$, unpaired Student t test). *D*: Serum levels of GIP, GLP-1, and PYY measured during an OGTT. Data are shown as mean ± SEM, $n \geq 5$ animals/group. Repeated-measures two-way ANOVA with Sidak multiple-comparison test, *$P < 0.05$. E-Cadh., E-Cadherin; TBP, TATA binding protein; rel., relative.

DISCUSSION

Insulin and IGF-I signaling play pivotal roles in metabolic homeostasis, embryonic development, and growth. Since both IR and IGF-IR have broad expression patterns, the specific functions of the IRs and IGF-IRs have been studied in a multitude of cell types and organs. However, the role of these receptors in one of the largest organs of the body, the intestine, has received relatively little attention.

Here we have investigated the role of the insulin and IGF-IRs on the development and function of the intestine by generating mice with an intestinal epithelial deletion of the IR (VILIRKO) and the IGF-IR (VILIGFRKO). Expression analyses of both receptors reveal the highest expression of the IR in the epithelium of the proximal small intestine with lower levels in the ileum, whereas levels in the colon were comparable to those in the duodenum. Conversely, IGF-IR expression is most highly expressed in the colon with lower expression in the proximal small intestine, suggesting nonredundant functions of these receptors in the intestine.

In contrast to what would have been anticipated from some previous studies (24,39,40), but in line with data on the intestinal IR by Andres et al. (23), the loss of neither the IR nor the IGF-IR impairs gut development or growth. However, as we did not study IR/IGF-IR double-knockout mice, we cannot exclude potential compensation during development or in very specific cellular functions. This lack of effect on growth suggests that concerns about oral insulin analogs having potential mitogenic and tumorigenic properties in the intestine are an unlikely safety concern and that the supplementation of infant formula with either IGF-I or insulin to improve gut maturation, as previously suggested (41), is also unlikely to provide major benefits.

Loss of the intestinal epithelial IR, however, does have some important, but unexpected, effects on glucose uptake from the intestinal lumen and release of the incretin GIP. Previous studies have provided conflicting results on the role of insulin action on glucose absorption. Some have reported insulin inhibition of glucose transport (42), whereas others have reported increased glucose entry into the enterocytes via a mechanism involving an increase in the numbers of glucose transporters (17). Unlike muscle and adipose tissue, where insulin-stimulated glucose uptake occurs through insulin-induced translocation of Glut4 from intracellular vesicles to the plasma membrane, intestinal glucose absorption is mediated primarily by SGLT1, which is constitutively localized to the apical brush border membrane. GLUT2, the other glucose transporter expressed in intestinal epithelial cells, primarily mediates the release of glucose into the circulation and has an additional role in glucose uptake at high luminal glucose concentrations (8,9). However, recent data using conditional deletion of GLUT2 in the intestinal epithelium revealed the effects of GLUT2 in reducing glucose uptake into the bloodstream and reducing body weight gain with only minor alterations in glucose tolerance (43). GIP levels were not assessed in that study, but the authors did find altered GLP-1–positive L-cell number without alterations in GLP-1 circulating levels.

In VILIRKO mice, there is no change in the expression of GLUT2 or the expression and localization of SGLT1 associated with the loss of insulin signaling, but there is a decrease in glucose transporter activity as measured in vivo and in vitro. Since attempts to assess alterations in GLUT2 protein either by Western blotting or immunofluorescent staining were inconclusive, the individual contribution of SGLT1 and GLUT2 to the observed phenotype remain to be determined; however, studies with the SGLT1 inhibitor phloridzin suggest that SGLT1 accounts for the majority of glucose uptake abnormality observed in the gut of VIKIRKO mice. Interestingly, the effect of IR deletion on reducing glucose absorption can be detected as early as 8 weeks of age, even though at that age no difference in oral glucose tolerance tests is observed. However, as a consequence of reduced intestinal glucose uptake, VILIRKO mice are protected from age- and HFD-induced glucose intolerance with no change in whole-body insulin sensitivity. Since villin-cre is also expressed in the epithelium of the proximal renal tubule, deleting the IR in these cells could impact glucose reabsorption. However, we did not detect any histological abnormalities in the kidneys, nor did Andres et al. in their study (23). Despite the reduced glucose absorption, we do not observe increased fecal caloric content in VILIRKO mice or any significant change in the community of gut microbiota.

We did, however, find that VILIRKO mice showed a selective reduction in GIP expression by both qPCR and Affymetrix analysis and a reduced number of GIP-positive cells. A similar reduction of GIP in intestinal epithelial IR knockouts was also observed in a previous study (23), although the observed GIP reduction in that study did not reach statistical significance. The reduced number of GIP-positive cells appears to be due to a reduction in the number of K-cells and/or a reduction in GIP expression in the K-cells. The fact that CHGA expression was unaltered in all small intestinal segments suggests no change in total enteroendocrine cell number, but a 20% reduction of GIP-positive cells. García-Martínez et al. (44) have shown that insulin can stimulate the expression of GIP in a glucose-dependent manner via the regulation of FoxO1 and LEF1/β-catenin. The reduced expression of GIP, combined with the dependence of GIP secretion on SGLT1 activity (9,45), leads to diminished secretion of GIP during acute glucose challenge. Previous studies (46) have shown that K-cell activation in response to an oral glucose challenge is strongly reduced in rats with type 2 diabetes. However, in this study, K-cells that were still responding to luminal glucose showed normal expression of GIP, whereas GLP-1 expression was reduced in L-cells from diabetic versus prediabetic rats, resulting in overall reduced GIP and even more pronounced GLP-1 expression. These data suggest that the IR knockout in the intestinal epithelium resembles the K-cell phenotype observed

in diabetic rats. However, elements of the diabetic phenotype, independent of the IR in intestinal epithelial cells, seem to regulate GLP-1 expression in L-cells.

Aside from its pharmacological role as an incretin, GIP also has effects on calcium homeostasis and bone remodeling as well as on lipid metabolism through the activation of lipoprotein lipase in adipocytes (45,47,48). The latter results in some protection of GIP-deficient mice from HFD-induced obesity (49). Consistent with this, the VILIRKO mice with reduced GIP release showed a slight, but not statistically significant, reduction of abdominal and visceral fat. They, however, had no change in bone mineral density as assessed using DEXA scans. Thus, the reduced GIP levels may play a role in insulin release but appear to be sufficient to mediate these other functions of this gastrointestinal hormone.

In summary, loss of the IR and IGF-IR in the intestinal epithelium has no influence on the development and proliferation of the intestinal epithelium, but loss of the IR does reduce intestinal glucose uptake through a decrease in glucose transporter activity, and this leads to beneficial metabolic effects, such as improved oral glucose tolerance with aging. Insulin action in the gut also controls K-cell number, and loss of the IR results in decreased numbers of K-cells and decreased levels of GIP. Thus, manipulating IR activity in the intestine could potentially provide long-term beneficial metabolic effects in aging and diabetes.

Funding. The Joslin Diabetes Research Center (DRC) Bioinformatics Core, which helped with data analysis, was supported by National Institutes of Health (NIH) grant P30-DK-036836, and the Brigham and Women's Hospital/Harvard Digestive Diseases Center for Clinical and Translational Metagenomics, which helped with microbiome analyses, was supported by NIH grant P30-DK-034854. This work was also supported by NIH grants DK-31036 to C.R.K. and DK-36836 to the Joslin DRC. S.U. is supported by iMed, the Helmholtz Initiative on Personalized Medicine. S.F. was supported by the Sunstar Foundation postdoctoral fellowship. The authors also thank the Mary K. Iacocca Professorship (C.R.K.) for their support.

Duality of Interest. No potential conflicts of interest relevant to this article were reported.

Author Contributions. S.U. and M.-F.H. wrote the manuscript and researched the data. S.F., D.L., and K.Y.L. researched the data and reviewed and edited the manuscript. N.L., G.K.G., and L.B. conducted the microbiome analyses. C.R.K. helped design experiments and edited the manuscript. C.R.K. is the guarantor of this work and, as such, had full access to all the data in the study and takes responsibility for the integrity of the data and the accuracy of the data analysis.

References

1. Louvard D, Kedinger M, Hauri HP. The differentiating intestinal epithelial cell: establishment and maintenance of functions through interactions between cellular structures. Annu Rev Cell Biol 1992;8:157–195

2. Perdue MH, McKay DM. Integrative immunophysiology in the intestinal mucosa. Am J Physiol 1994;267:G151–G165

3. Depoortere I. Taste receptors of the gut: emerging roles in health and disease. Gut 2014;63:179–190

4. Raja M, Puntheeranurak T, Hinterdorfer P, Kinne R. SLC5 and SLC2 transporters in epithelia-cellular role and molecular mechanisms. Curr Top Membr 2012;70:29–76

5. Iqbal J, Hussain MM. Intestinal lipid absorption. Am J Physiol Endocrinol Metab 2009;296:E1183–E1194

6. Macfarlane GT, Macfarlane S. Human colonic microbiota: ecology, physiology and metabolic potential of intestinal bacteria. Scand J Gastroenterol Suppl 1997;222:3–9

7. Takata K, Kasahara T, Kasahara M, Ezaki O, Hirano H. Immunohistochemical localization of Na(+)-dependent glucose transporter in rat jejunum. Cell Tissue Res 1992;267:3–9

8. Gorboulev V, Schürmann A, Vallon V, et al. Na(+)-D-glucose cotransporter SGLT1 is pivotal for intestinal glucose absorption and glucose-dependent incretin secretion. Diabetes 2012;61:187–196

9. Röder PV, Geillinger KE, Zietek TS, Thorens B, Koepsell H, Daniel H. The role of SGLT1 and GLUT2 in intestinal glucose transport and sensing. PLoS One 2014;9:e89977

10. Drucker DJ. The biology of incretin hormones. Cell Metab 2006;3:153–165

11. Hediger MA, Rhoads DB. Molecular physiology of sodium-glucose cotransporters. Physiol Rev 1994;74:993–1026

12. Boucher J, Kleinridders A, Kahn CR. Insulin receptor signaling in normal and insulin-resistant states. Cold Spring Harb Perspect Biol 2014;6:a009191

13. Manome S, Kuriaki K. Effect of insulin, phlorizin and some metabolic inhibitors on the glucose absorption from the intestine. Arch Int Pharmacodyn Ther 1961;130:187–194

14. Aulsebrook KA. Intestinal transport of glucose and sodium: changes in alloxan diabetes and effects of insulin. Experientia 1965;21:346–347

15. Gottesbüren H, Schmitt E, Menge H, Bloch R, Lorenz-Meyer H, Riecken EO. The effect of insulin on the intestinal absorption in man. I. Absorption of glucose, water and electrolytes in diabetics and healthy controls. Res Exp Med (Berl) 1973;160:326–330 [in German]

16. Costrini NV, Ganeshappa KP, Wu W, Whalen GE, Soergel KH. Effect of insulin, glucose, and controlled diabetes mellitus on human jejunal function. Am J Physiol 1977;233:E181–E187

17. Serhan MF, Kreydiyyeh SI. Insulin down-regulates the Na+/K+ ATPase in enterocytes but increases intestinal glucose absorption. Gen Comp Endocrinol 2010;167:228–233

18. Arsenault P, Ménard D. Insulin influences the maturation and proliferation of suckling mouse intestinal mucosa in serum-free organ culture. Biol Neonate 1984;46:229–236

19. Howarth GS. Insulin-like growth factor-I and the gastrointestinal system: therapeutic indications and safety implications. J Nutr 2003;133:2109–2112

20. Dupont J, Holzenberger M. Biology of insulin-like growth factors in development. Birth Defects Res C Embryo Today 2003;69:257–271

21. Liu JP, Baker J, Perkins AS, Robertson EJ, Efstratiadis A. Mice carrying null mutations of the genes encoding insulin-like growth factor I (Igf-1) and type 1 IGF receptor (Igf1r). Cell 1993;75:59–72

22. Rubin R, Baserga R. Insulin-like growth factor-I receptor. Its role in cell proliferation, apoptosis, and tumorigenicity. Lab Invest 1995;73:311–331

23. Andres SF, Santoro MA, Mah AT, et al. Deletion of intestinal epithelial insulin receptor attenuates high-fat diet-induced elevations in cholesterol and stem, enteroendocrine, and Paneth cell mRNAs. Am J Physiol Gastrointest Liver Physiol 2015;308:G100–G111

24. Rowland KJ, Trivedi S, Lee D, et al. Loss of glucagon-like peptide-2-induced proliferation following intestinal epithelial insulin-like growth factor-1-receptor deletion. Gastroenterology 2011;141:2166–2175.e7

25. Gautier L, Cope L, Bolstad BM, Irizarry RA. affy–analysis of Affymetrix GeneChip data at the probe level. Bioinformatics 2004;20:307–315

26. Durinck S, Spellman PT, Birney E, Huber W. Mapping identifiers for the integration of genomic datasets with the R/Bioconductor package biomaRt. Nat Protoc 2009;4:1184–1191

27. Booth C, O'Shea JA. Isolation and Culture of Intestinal Epithelial Cells. In *Culture of Epithelial Cells*. 2nd ed. Freshney RI, Freshney MG, Eds. New York, Wiley-Liss, 2002, p. 303–335

28. Kozich JJ, Westcott SL, Baxter NT, Highlander SK, Schloss PD. Development of a dual-index sequencing strategy and curation pipeline for analyzing amplicon sequence data on the MiSeq Illumina sequencing platform. Appl Environ Microbiol 2013;79:5112–5120

29. Schloss PD, Westcott SL, Ryabin T, et al. Introducing mothur: open-source, platform-independent, community-supported software for describing and comparing microbial communities. Appl Environ Microbiol 2009;75:7537–7541
30. Shannon C, Weaver W. *The Mathematical Theory of Communication*. Urbana, IL, University of Illinois Press, 1963
31. McMurdie PJ, Holmes S. phyloseq: an R package for reproducible interactive analysis and graphics of microbiome census data. PLoS One 2013;8:e61217
32. McMurdie PJ, Holmes S. Waste not, want not: why rarefying microbiome data is inadmissible. PLoS Comput Biol 2014;10:e1003531
33. el Marjou F, Janssen KP, Chang BH, et al. Tissue-specific and inducible Cre-mediated recombination in the gut epithelium. Genesis 2004;39:186–193
34. Freier S, Eran M, Reinus C, et al. Relative expression and localization of the insulin-like growth factor system components in the fetal, child and adult intestine. J Pediatr Gastroenterol Nutr 2005;40:202–209
35. Gallo-Payet N, Hugon JS. Insulin receptors in isolated adult mouse intestinal cells: studies in vivo and in organ culture. Endocrinology 1984;114:1885–1892
36. Watanabe M, Hayasaki H, Tamayama T, Shimada M. Histologic distribution of insulin and glucagon receptors. Braz J Med Biol Res 1998;31:243–256
37. Wright EM, Turk E, Hager K, et al. The Na+/glucose cotransporter (SGLT1). Acta Physiol Scand Suppl 1992;607:201–207
38. Shirazi-Beechey SP, Moran AW, Batchelor DJ, Daly K, Al-Rammahi M. Glucose sensing and signalling; regulation of intestinal glucose transport. Proc Nutr Soc 2011;70:185–193
39. Qiu W, Leibowitz B, Zhang L, Yu J. Growth factors protect intestinal stem cells from radiation-induced apoptosis by suppressing PUMA through the PI3K/AKT/p53 axis. Oncogene 2010;29:1622–1632
40. Suman S, Kallakury BV, Fornace AJ Jr, Datta K. Protracted upregulation of leptin and IGF1 is associated with activation of PI3K/Akt and JAK2 pathway in mouse intestine after ionizing radiation exposure. Int J Biol Sci 2015;11:274–283
41. Shamir R, Shehadeh N. Insulin in human milk and the use of hormones in infant formulas. Nestle Nutr Inst Workshop Ser 2013;77:57–64
42. Pennington AM, Corpe CP, Kellett GL. Rapid regulation of rat jejunal glucose transport by insulin in a luminally and vascularly perfused preparation. J Physiol 1994;478:187–193
43. Schmitt CC, Aranias T, Viel T, et al. Intestinal invalidation of the glucose transporter GLUT2 delays tissue distribution of glucose and reveals an unexpected role in gut homeostasis. Mol Metab 2017;6:61–72
44. García-Martínez JM, Chocarro-Calvo A, De la Vieja A, García-Jiménez C. Insulin drives glucose-dependent insulinotropic peptide expression via glucose-dependent regulation of FoxO1 and LEF1/beta-catenin. Biochim Biophys Acta 2014;1839:1141–1150
45. Yabe D, Seino Y. Incretin actions beyond the pancreas: lessons from knockout mice. Curr Opin Pharmacol 2013;13:946–953
46. Lee J, Cummings BP, Martin E, et al. Glucose sensing by gut endocrine cells and activation of the vagal afferent pathway is impaired in a rodent model of type 2 diabetes mellitus. Am J Physiol Regul Integr Comp Physiol 2012;302:R657–R666
47. Tsukiyama K, Yamada Y, Yamada C, et al. Gastric inhibitory polypeptide as an endogenous factor promoting new bone formation after food ingestion. Mol Endocrinol 2006;20:1644–1651
48. Furusawa Y, Obata Y, Hase K. Commensal microbiota regulates T cell fate decision in the gut. Semin Immunopathol 2015;37:17–25
49. Miyawaki K, Yamada Y, Ban N, et al. Inhibition of gastric inhibitory polypeptide signaling prevents obesity. Nat Med 2002;8:738–742